Probing the Effects of Membrane Cholesterol in the *Torpedo californica* Acetylcholine Receptor and the Novel Lipid-exposed Mutation αC418W in *Xenopus* Oocytes*

John Santiago‡§, Gisila R. Guzmán‡, Legier V. Rojas¶, Ricardo Marti‡, Guillermo A. Asmar-Rovira‡, Luis F. Santana‖, Mark McNamee**, and José A. Lasalde-Dominicci‡ ‡‡

*From the ‡Department of Biology, University of Puerto Rico, P. O. Box 23360, San Juan, Puerto Rico 00931-3360, the ‖Institute of Neurobiology, 201 Blvd. del Valle, Old San Juan, Puerto Rico 00901, the ¶Department of Physiology, School of Medicine, Universidad Central del Caribe, Bayamon, Puerto Rico 00960-6032, and the **Section of Molecular and Cellular Biology, University of California, Davis, California 95616*

The effects of cholesterol on the ion-channel function of the *Torpedo* acetylcholine receptor (nAChR) and the novel lipid-exposed gain in function αC418W mutation have been investigated in *Xenopus laevis* oocytes. We found conditions to increase the cholesterol/phospholipid (C/P) molar ratio on the plasma membrane of *Xenopus* oocytes from 0.5 to 0.87, without significant physical damage or change in morphology to the oocytes. In addition, we developed conditions to deplete endogenous cholesterol from oocytes using a methyl-β-cyclodextrin incubation procedure without causing membrane instability of the cells. Methyl-β-cyclodextrin was also used to examine the reversibility of the inhibitory effect of cholesterol on AChR function. Depletion of 43% of endogenous cholesterol from oocytes (C/P = 0.3) did not show any significant change in macroscopic response of the wild type, whereas in the αC418W mutant the same cholesterol depletion caused a dramatic gain-in-function response of this lipid-exposed mutation in addition to the increased response caused by the mutation itself. Increasing the C/P ratio to 0.87 caused an inhibition of the macroscopic response of the *Torpedo* wild type of about 52%, whereas the αC418W mutation showed an 81% inhibition compared with the responses of control oocytes. The wild type receptor did not recover from this inhibition when the excess cholesterol was depleted to near normal C/P ratios; however, the αC418W mutant displayed 63% of the original current, which indicates that the inhibition of this lipid-exposed mutant was significantly reversed. The ability of the αC418W mutation to recover from the inhibition caused by cholesterol enrichment suggests that the interaction of cholesterol with this lipid-exposed mutation is significantly different from that of the wild type. The present data demonstrate that a single lipid-exposed position in the AChR could alter the modulatory effect of cholesterol on AChR function.

The nicotinic acetylcholine receptor (nAChR)[1] from muscle and electric ray organ is an integral membrane protein comprised of four homologous polypeptide subunits in a stoichiometry of $\alpha_2\beta\gamma\delta$ (for review see Refs. 1–6). A consensus model for the nAChR topology deduced from hydrophobicity profiles for protein sequences obtained from cDNA sequences indicates that each subunit contains at least four membrane-spanning regions denoted M1 through M4 with both N and C termini located on the extracellular side (7). This integral membrane protein has been extensively used for the study of lipid-protein interactions.

Previous biophysical studies of the nAChR used cholesterol as a probe for the study of lipid-protein interactions. Most of the information available on the sensitivity of the nAChR to the lipid environment was obtained using reconstituted membranes of purified *Torpedo californica* AChR. However, despite a wealth of experimental data from reconstituted systems, the role of membrane cholesterol in regulating AChR function has not been completely elucidated, and some of the results have remained controversial and sometimes even contradictory. The contradictory results in the literature regarding the specific lipid requirements of the nAChR may reflect a variety of conditions, including the fact that the functional status of the nAChR in most cases was performed in reconstituted membranes with the additional lipid of interest tested at a molar percentage of the total membrane lipids different from the natural membranes. The relative level of a given lipid may be the key factor in determining the fraction of AChR in a functional conformation as well as the kinetics of the conformational change.

In reconstituted membranes, the ability of the nAChR to conduct cations across the membrane and to undergo conformational transitions from the resting to the desensitized state $(R \Rightarrow D)$ has been shown to be very sensitive to the lipid composition (8–10). The mechanism by which lipid modulates the ability of nAChR to undergo an agonist-induced conformational change remains unclear. A previous proposal suggested the possibility that cholesterol regulation of membrane fluidity might play a key role in the modulation of AChR function (9); however, subsequent work challenged the fluidity hypothesis (11, 12). A recent Fourier transform infrared study using reconstituted membranes of purified nAChR raised the fluidity hypothesis again (13). This study proposed that the membrane fluidity modulates the relative population of nAChRs in the

[1] The abbreviations used are: nAChR, nicotinic acetylcholine receptor; C/P, cholesterol/phospholipid molar ratio.

resting and desensitized states. The data from reconstitution experiments demonstrated that cholesterol interacts at some discrete class of binding sites on the receptor (14, 15). Recently, the binding sites for cholesterol at the protein interface of the *Torpedo* nAChR were mapped using a novel photoreactive analog of cholesterol (^{125}I-azido-cholesterol) (16). This study found that cholesterol-binding sites were exclusive to the alpha M4 and M1 and gamma M4 transmembrane segments. The binding kinetics of ethidium bromide to the reconstituted *Torpedo nobiliana* nAChR suggest that in the absence of cholesterol the receptor is "locked" in the R conformation (17, 18). Rankin and coworkers (17) showed that the number of nAChRs that open in response to high agonist concentrations increase with the percentage of cholesterol in the bilayer, reaching a maximum at 30 mol% of cholesterol. This value corresponds to a C/P molar ratio of about 0.42 that is slightly lower than the molar ratio that we found in the *Xenopus oocyte* plasmatic membrane.

In the present work we manipulate the cholesterol/phospholipid molar ratios in the oocyte membrane to reach higher membrane cholesterol levels (C/P = 0.87) than the ratios studied in the reconstituted system. We also depleted endogenous cholesterol from oocytes to reach C/P molar ratios similar to the ones previously examined in the reconstituted system. The voltage clamp technique was used to examine the effect of cholesterol on *T. californica* nAChR function, including the effect on a novel lipid-exposed αC418W mutation that has been shown to increase the macroscopic response (19–21). Our data show that the interaction of cholesterol with *Torpedo* wild type is remarkably different from the interaction with the αC418W mutant. These results raise the importance of the functional role of lipid-protein interactions in ion-channel function and underscore the importance of cysteine 418 in the α subunit of the *Torpedo* nAChR in the modulatory action of cholesterol. This approach will open a new dimension for studying lipid effects on ion-channel function.

EXPERIMENTAL PROCEDURES

Confocal Imaging—The time course of cholesterol incorporation into oocytes was monitored using a fluorescent cholesterol analog (22-(*N*-(7-nitrobenz-2-oxa-1,3-diazol-4-yl)amino)-23,24-bisnor-5-cholen-3-ol; Molecular Probes, Eugene, OR) and a Bio-Rad MRC-600 confocal system, coupled to a Nikon Diaphot inverted microscope equipped with a 20× objective (numerical aperture = 0.5, Olympus). This cholesterol analog was excited with the 469-nm line of a Kr/Ar laser while its emission was monitored through one of the two acquisition channels of the MRC-600 using the appropriate set of filters.

Isolation of the Plasma Membranes—The isolation of the plasma membranes of the oocyte was accomplished according to a procedure as described previously (22) with minor modifications. The vitelline membranes of 15 oocytes were removed manually, and a homogenate was layered on top of a 0.5 volume of 1.5 M sucrose (in 20 mM Tris-HCl, pH 7.6, 10 mM MgCl$_2$, 50 mM KCl, 2 mM 2-mercaptoethanol, 1 mM EGTA, 0.1 mM phenylmethylsulfonyl fluoride) and centrifuged. The fatty layer was discarded, the membranes were retrieved from the interface between the two layers, diluted with 4 volumes of buffer B (5.0 mM Hepes, pH 7.4, 0.16 M NaCl, 0.1 mM phenylmethylsulfonyl fluoride), and pelleted at 16,000 × *g* 10 min, at 4 °C. Cholesterol/phospholipid (C/P) molar ratio of the plasmatic membrane of the oocyte was estimated using protocols as described (23, 24).

Preparation of Cholesterol-enriched Liposomes—Liposomes were prepared using the detergent removal technique and a Mini Lipoprep (Amika Corp. catalog number S81110D). A solution containing cholesterol/phosphatidylcholine/cholate at a molar ratio 1:1:2 was prepared in chloroform. The mixed micelles formed spontaneously when lipids and detergent deposited from the organic solvent are exposed to the MOR2 buffer. A lipid:detergent molar ratio of 0.8 was used, and the exposure of lipids to the aqueous solvent was performed above the transition temperature of the lipids. Subsequently, detergent removal was accomplished at constant temperature using the Mini-Lipoprep-Dialyzer (volume capacity 1.0 ml) and a DIACHEMA membrane (10.1 molecular weight cut-off 10,000, high permeability). The resulting unilamellar

liposomes are well-defined tailored vesicles in the diameter size range of 50–200 nm.

Estimation of C/P Molar Ratios in the Plasma Membrane of Oocytes—Briefly, ten sample of 50 μl containing the plasma membrane are dried using nitrogen gas. Five of the samples were used for the cholesterol molar estimation, and the other five were used for the phospholipid molar estimation. For the cholesterol concentration, the five samples were resuspended in 50 μl of Infinity cholesterol reagent (Sigma Chemical Co., St. Louis, MO, catalog number 40125p) and incubated at 37 °C for 5 min. The cholesterol concentration (milligrams/dl) of the samples was estimated by spectrophotometry at 501 nm. For the phospholipid concentration, the samples are resuspended in 50 μl of the saponification solution (2.0 M KOH in methanol) and incubated at room temperature for 2 h. After the incubation 500 μl of the molybdenum solution was added (1 ml of 5% molybdenum, 3 ml of 15% ascorbic acid, 6 ml of dephosphorylated water) and incubated at 50 °C for 10 min. The phospholipid concentration was estimated by spectrophotometry at 820 nm. The cholesterol:phospholipid molar ratio of the plasma membrane of oocytes was estimated using the methods as described (23, 24).

Cholesterol Depletion Experiments in Intact Oocytes—Cholesterol depletion in oocytes was accomplished using the procedure as described previously (25) with some modifications. Briefly, oocytes were incubated in 300 μl of 50 μM methyl-β-cyclodextrin for 45 min and then washed three times with a total volume of 3 ml of MOR2. This water-soluble cyclic oligosaccharide has a high affinity for cholesterol and has been heavily used as an effective tool for the transport of cholesterol away from the cell surface (26). We used these protocols to deplete endogenous cholesterol from oocytes and also to remove a fractional amount of the excess of cholesterol after enrichment.

Cholesterol Enrichments Protocol—Cholesterol was incorporated into *Xenopus* oocytes in a reversible manner as follows. The oocytes were incubated in a solution containing cholesterol-enriched liposomes at room temperature for 45 min. The incubated oocytes were then washed three times with a total volume of 3 ml of MOR2. The cholesterol/phospholipid (C/P) molar ratio of the plasma membrane of the oocytes was estimated using protocols as described (23, 24) with minor modification as described (27, 28). This method increased the cholesterol phospholipid molar ratio of plasma membrane of the oocyte from 0.51 ± 0.1 (control) to 0.87 ± 0.06 (n = 90 oocytes in six batches of oocytes). The average percentage of enrichment was 71%, and the C/P molar ratios of the enriched oocytes were in the range 0.78–0.97.

Depletion of Cholesterol-enriched Oocytes—Oocytes expressing wild type or the αC418W mutant were perfused with 100 μM ACh and then exposed to a 45-min period of cholesterol enrichment. After cholesterol enrichment, oocytes were voltage-clamped, and the macroscopic response was assessed again with 100 μM ACh (another experimental protocol was to perform a dose-response curve 1–300 μM ACh). Subsequently, oocytes were exposed to methyl-β-cyclodextrin (50 μM) for 45 min and then washed three times with 3 ml of MOR2, voltage-clamped, and perfused with 100 μM ACh. Control experiments were performed following the same protocols using MOR2 without methyl-β-cyclodextrin.

Expression in X. laevis Oocytes—RNA transcripts were synthesized *in vitro* as described previously (19). The RNA transcripts (10 ng/oocyte at the concentration of 0.2 μg/μl) of α, β, γ, and δ subunit at a 2:1:1:1 ratios were injected into *Xenopus* oocytes.

Voltage Clamping—ACh-induced currents were recorded with a two-electrode voltage clamp 3–5 days after mRNA injection with the Gene Clamp 500 amplifier (Axon Instruments, Foster City, CA). Electrodes were filled with 3 M KCl and had resistance of less than 2 MΩ. Impaled oocytes in the recording chamber were perfused at a rate of 0.5 ml/s with MOR2 buffer (115 mM NaCl, 2.5 mM KCl, 5 mM MgCl$_2$, 1 mM Na$_2$HPO$_4$, 5 mM HEPES, 0.2 mM CaCl$_2$, pH 7.4). ACh solutions were made from calcium-free MOR2 to avoid activation of an endogenous Ca^{2+}-dependent Cl$^-$ current (29, 30). For dose-response curves, each oocyte was held at a membrane potential of −70 mV. Membrane currents were digitized at 0.5–2 kHz and filtered at 0.1 kHz using a TL-1 interface (Axon Instruments) and acquired by Whole Cell Program 3.2.1 software (kindly provided by Dr. John Demspter) running on a Pentium III-based computer. Prisma version 3.0 (GraphPad, San Diego, CA) software were utilized for data analysis and fitting. Dose-response data were collected from peak currents at six ACh concentrations in the range of 1.0 to 300 μM. The data were fit using a curve of the form $Y = 100/[1 + (EC_{50}/A)^n]$ and non-linear regression curves. The EC$_{50}$ values for individual oocytes were averaged to generate final estimates.
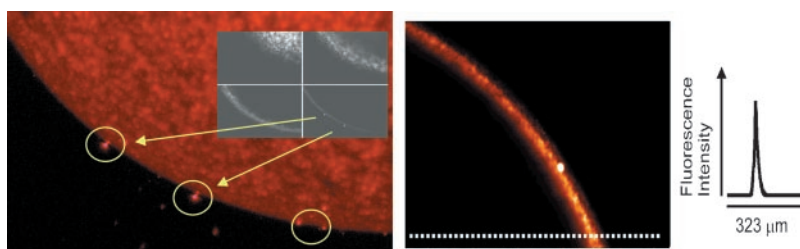
FIG. 1. **Cholesterol enrichment in the plasma membrane of** *X. laevis* **oocytes monitored with confocal imaging.** Image reconstruction of 32 sequential confocal images showing incorporation of a fluorescent cholesterol analog (22-(*N*-(7-nitrobenz-2-oxa-1,3-diazol-4-yl)amino)-23,24-bisnor-5-cholen-3-ol) to the surface of a *X. laevis* oocyte. Liposomes containing the fluorescent cholesterol analog (*inside yellow circles*) are shown fusing with the plasma membrane (*left*). In the insert, 4 of a total of 32 sections are shown (*right*). Images were acquired using a Bio-Rad MRC 600 confocal microscope coupled to a Nikon Diaphot inverted microscope using a 20× objective (numerical aperture = 0.5; Olympus). Confocal sections were taken at intervals of 10 μm. Note that if one focuses the confocal microscope toward the center of the cell, a donut-like fluorescent pattern characteristic of fluorophores targeted to the plasma membrane could be observed. Indeed, from plots of the fluorescence intensity along the *dotted line* in the *middle panel* it is clear that the fluorescence is restricted to the surface membrane. Note, however, that the spatial profile of this membrane-associated fluorophore depends on the thickness of each confocal section. As the thickness of the section is increased, more out-of-focus fluorescence will contribute to the collected image. Thus, the thickness of the fluorescence intensity profile (*left-most panel*) could give the impression to the reader that the membrane at this section is thicker than it actually is.
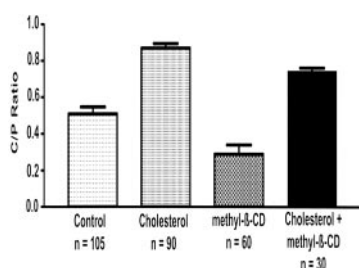

FIG. 2. **Estimation of cholesterol/phospholipid (C/P) molar ratios.** For each experiment 15 oocytes were used. For the control oocytes the calculated C/P molar ratio average in seven experiments ($n = 105$ oocytes) was 0.51. After cholesterol enrichment the C/P molar ratio average was 0.87 (six experiments, $n = 90$ oocytes). For cholesterol-depleted oocytes the C/P molar ratio had an average of 0.3 (four experiments, $n = 60$ oocytes). In oocytes that were incubated with methyl-β-cyclodextrin after cholesterol enrichment, there was a reduction of 0.12 in the C/P molar ratio with a final average of 0.75. Note that the differences were calculated based on the evaluation of the control oocytes.

RESULTS

We began our study of the effects of cholesterol on the function of the acetylcholine receptor by developing a strategy to dynamically change the cholesterol levels in the surface of *X. laevis* oocytes. We took advantage of a recently developed fluorescent cholesterol analog (22-(*N*-(7-nitrobenz-2-oxa-1,3-diazol-4-yl)amino)-23,24-bisnor-5-cholen-3-ol) to monitor cholesterol incorporation into the surface membrane of cells following the incubation with cholesterol-enriched liposomes using a confocal microscope (Fig. 1). An important consideration in these studies was to significantly enrich the surface membrane of cells without altering intracellular cholesterol concentration. A series of confocal sections of an oocyte exposed to the liposomes containing the cholesterol fluorescent analog are shown in Fig. 1 (*left*). We found that under our controlled conditions cholesterol was preferentially incorporated into the plasma membrane (Fig. 1, *right*). Using this approach we estimated the approximate time of liposome exposure required to reach a cholesterol to phospholipid molar ratio (C/P) of 0.87.

Cholesterol Enrichment and AChR Function—The cholesterol/phospholipid molar ratio of the plasma membrane of oocytes was in the range of 0.33–0.62 in seven batches of oocytes tested, and the mean value obtained was 0.51 ± 0.10 (Fig. 2). However, there seems to be variability in the C/P molar ratio that appears to be seasonal. As shown in Fig. 2, the enrichment produced oocytes with a C/P molar ratio in the order of 0.87. This C/P molar ratio is higher than the molar ratios reported in reconstitution experiments of the *T. californica* AChR (17). The
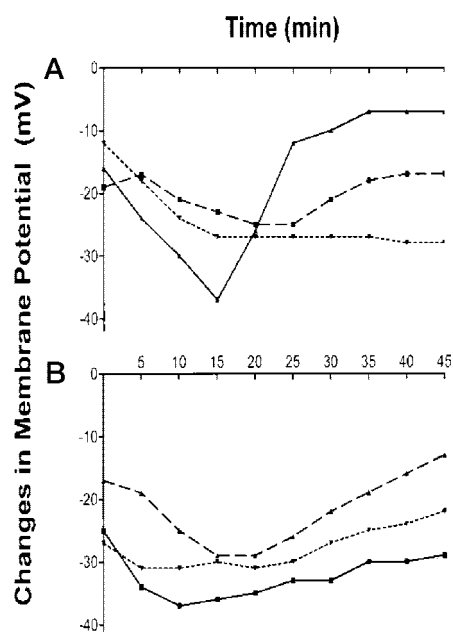

FIG. 3. **Membrane potential changes during cholesterol enrichment or depletion.** Membrane potential was monitored during 45 min of cholesterol enrichment (*A*) or cholesterol depletion (*B*); ($n = 3$ oocytes in both cases). During cholesterol enrichment the membrane potential shifted with a biphasic behavior. First a moderate decrease in the range of 10–15 mV during the first 15 min was followed by a slow membrane repolarization (*A*). Cholesterol depletion caused a moderate decrease in the membrane potential of oocytes during the first 15 min of methyl-β-cyclodextrin exposure that was in the range of 10–15 mV. After 20 min of methyl-β-cyclodextrin exposure, the oocytes gradually recovered their membrane potential (*B*).

resting membrane potential of the oocytes was only modestly affected during the 45-min period of cholesterol enrichment (Fig. 3*A*). The shift in membrane potential was overcome by voltage-clamping oocytes at −70 mV for measuring nAChR currents. The moderate hyperpolarization observed during the first 15 min could be caused by an inhibitory effect of cholesterol on the membrane-bound pumps, which are responsible for the upkeep of the underlying ionic gradients. Interestingly, we observed that in almost all the cholesterol-enriched oocytes, exposure to methyl-β-cyclodextrin restored the membrane potential by inducing a hyperpolarization that was in the range of −5 to −20 mV. Thus, under the conditions that we used, cholesterol seems to play a modulatory role in maintaining the resting membrane potential of the oocyte. Fig. 4*A* shows three typical experimental results in which an oocyte was voltage-
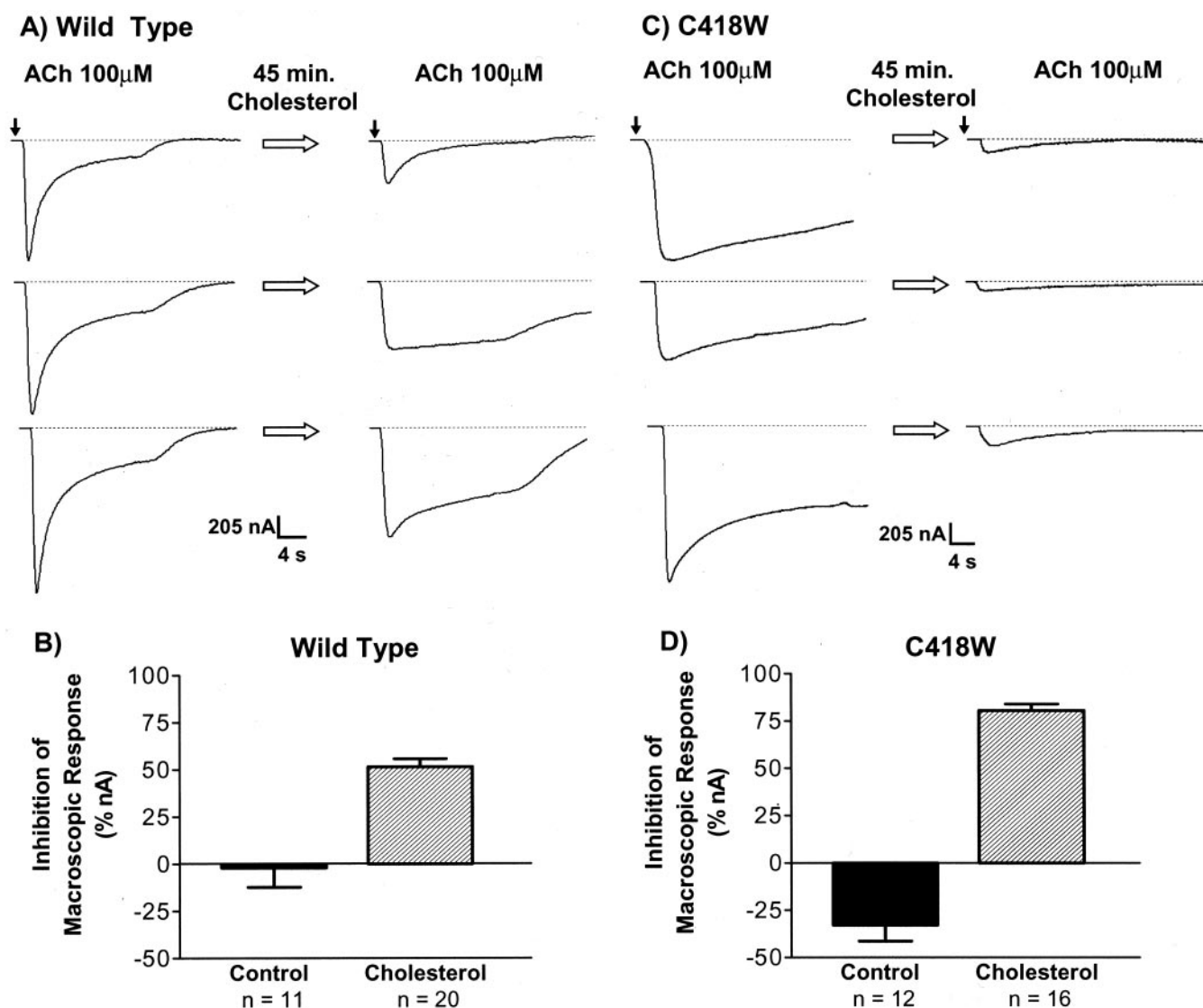
Cholesterol and Acetylcholine Receptor

A) Wild Type

ACh 100μM   45 min.   ACh 100μM
                   Cholesterol

C) C418W

ACh 100μM   45 min.   ACh 100μM
                   Cholesterol

205 nA└
    4 s

205 nA└
    4 s

B) **Wild Type**

Inhibition of Macroscopic Response (% nA)

Control n = 11   Cholesterol n = 20

D) **C418W**

Inhibition of Macroscopic Response (% nA)

Control n = 12   Cholesterol n = 16

FIG. 4. **Cholesterol enrichment produces an inhibitory response of the AChR.** *A* and *C*, representative current traces of three different oocytes for the wild type (*WT*) and the mutant αC418W, before and after cholesterol enrichment. The oocytes were perfused with 100 μM ACh and incubated with cholesterol liposomes for 45 min. After the incubation, oocytes were washed three times with 1 ml of MOR2 and perfused again with 100 μM ACh. In both cases there was an inhibition of the macroscopic response after cholesterol enrichment; this inhibition was more dramatic in the mutant αC418W. *B* and *D*, average percentages of inhibition of WT and αC418W AChR after cholesterol enrichment. There was a 51.5% of inhibition of WT ($n = 20$) and 80.5% on the αC418W ($n = 16$). In both cases the controls were oocytes that were incubated with MOR2 for 45 min instead of the cholesterol-enriched liposome.

clamped at -70 mV and perfused with 100 μM acetylcholine (ACh) before (*left*) and after (*right*) cholesterol enrichment. In cholesterol-enriched oocytes (C/P = 0.87) the *Torpedo* wild type AChR displays a macroscopic current inhibition of about 51.5% ($n = 20$) compared with the control oocytes. Fig. 4*C* shows the same experiment for the lipid-exposed mutation αC418W, and the same cholesterol enrichment protocol leads to a 80.5% inhibition ($n = 16$ oocytes) for this mutation. This result indicates that the functional response of the αC418W is more sensitive to the presence of higher levels of cholesterol in the plasma membrane than the wild type. Fig. 4*B* represents an average of the response of control oocytes that were incubated in MOR2 only for the 45 min of incubation (*i.e.* no added cholesterol present). The macroscopic current was recorded at -70 mV with 100 μM ACh as in the enriched oocyte. This control was performed to subtract the current that appears in the absence of cholesterol that might be due to an apparent gain-in-function due to the assembly of new surface nAChRs. As shown in Fig. 4 (*B* and *D*) the negative percentage of inhibition of the macroscopic response represents an increase in the

current. This means that, after exposing the oocyte for the first time to ACh, there is a very small increase in the wild type response (2%) response whereas in the αC418W the response is higher (33%) than for the wild type. If the αC418W produced a higher response after the first exposure to ACh, this suggests that the inhibition of this mutation could be even higher than the 80.5% detected in our protocol. Fig. 5*A* shows a family of macroscopic currents from oocytes expressing the αC418W mutant before (*left*) and after cholesterol enrichment (*right*). The dose-response curves for the control and cholesterol-enriched oocytes expressing the αC418W are shown in Fig. 5*B*. From the reduction in the macroscopic response, it is clear that cholesterol produced a substantial inhibitory response for the αC418W, however; the EC_{50} for ACh seems to be similar after the enrichment. Fig. 5*C* shows a family of macroscopic currents for an oocyte expressing wild type before (*left*) and after cholesterol enrichment (*right*). The dose-response curves for the normal and cholesterol-enriched oocytes expressing wild type are shown in Fig. 5*D*. The EC_{50} values for the inhibited state in the cholesterol-enriched oocyte appear to be similar to the
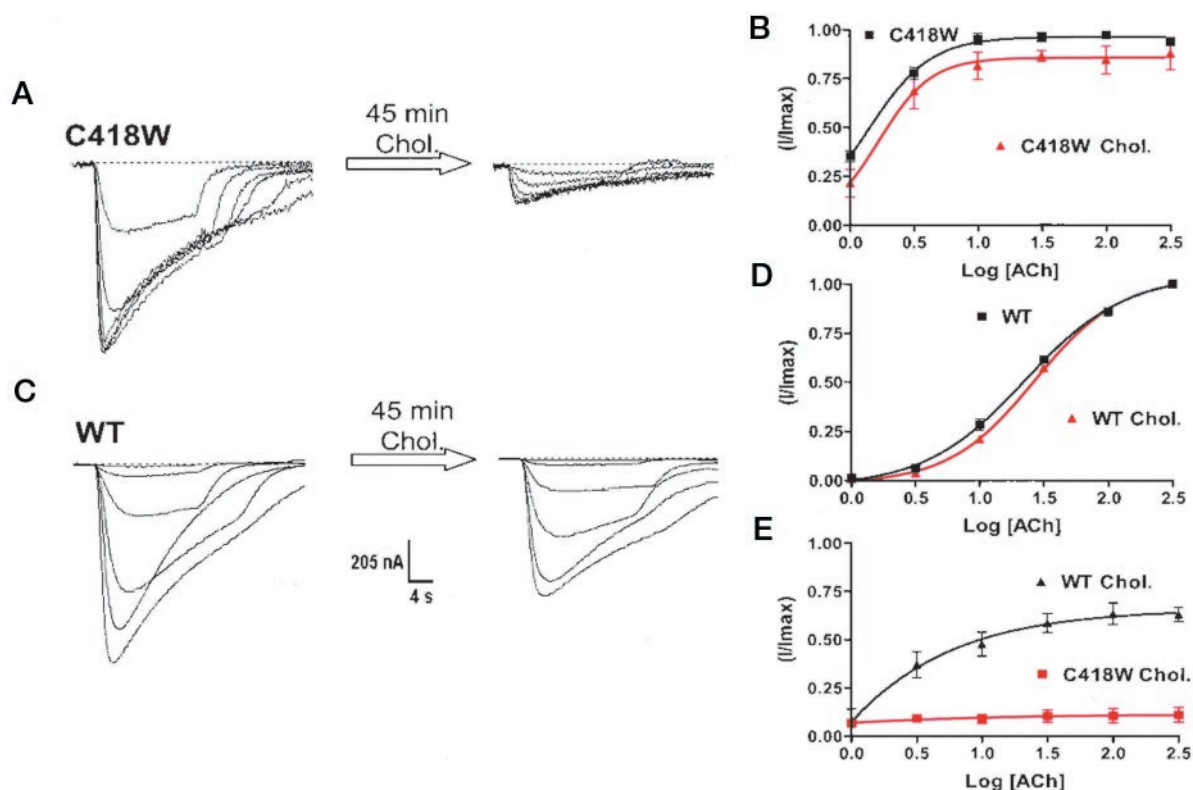
FIG. 5. **Cholesterol enrichment does not affect the EC$_{50}$ of the AChR.** Families of macroscopic current traces for the αC418W and WT before and after cholesterol enrichment are shown in *A* and *C*, respectively. The ACh concentrations used for the generation of the family of currents were 1.0, 3.0, 10, 30, 100, and 300 μM. Oocytes were clamped at −70 mV. After cholesterol enrichment (C/P = 0.87) the dose-response curves for the αC418W (*B*) and WT (*D*) remain similar to the control. The EC$_{50}$ of the αC418W (*n* = 3) was 2.7 ± 0.6 μM before and 2.3 ± 0.1 μM after cholesterol enrichment. For the WT (*n* = 3) the EC$_{50}$ was 22.6 ± 0.2 μM before and 27.2 ± 0.5 μM after cholesterol enrichment. ACh-induced currents of the cholesterol-enriched oocytes (*right currents*) are normalized to the equivalent ACh-induced currents previous to the cholesterol enrichment (*left current traces*). Data from three to six different oocytes were normalized to provide a statistical average of the decrease in macroscopic response for the WT and αC418W mutant (*E*).

control experiments for wild type and the αC418W, suggesting that the loss in functional response could be due to a reduction in the number of resting nAChR rather than an inhibitory effect on the ion-channel function. To estimate the overall reduction in the macroscopic response, ACh-induced currents of cholesterol-enriched oocytes were normalized to the equivalent maximum current of control oocytes. As shown in Fig. 5*E*, after cholesterol enrichment, the wild type displayed a fraction of 0.62 of the original current at the highest ACh concentration used, whereas for the αC418W mutant only about 0.1 of the original current was detected after the enrichment.

Cholesterol Depletion Experiments—These experiments were designed to examine the functional response of the *Torpedo* wild type and αC418W mutant in a reduced cholesterol environment. The resting membrane potential and the physical condition of oocytes were not affected during the methyl-β-cyclodextrin incubation period. During cholesterol depletion we observed a moderate hyperpolarization in the membrane potential of oocytes during the first 15 min that was in the range of 10–15 mV. However, after 25 min the potential gradually recovered (Fig. 3*B*). After the depletion protocol, oocytes showed C/P molar ratios in the range of 0.19–0.44; the average C/P obtained in 11 batches of oocytes tested was 0.3 ± 0.1 (*n* = 60 oocytes tested) as shown in Fig. 2. Oocytes expressing wild type and the αC418W mutant were perfused with 100 μM ACh and then exposed to methyl-β-cyclodextrin (50 μM) in MOR2 for 45 min. Immediately after incubation oocytes were washed, voltage-clamped, and perfused with 100 μM ACh. Macroscopic currents from a representative experiment are shown in Fig. 6 (*A–D*). Fig. 6*A* shows one control experiment in which an oocyte is voltage-clamped at −70 mV and perfused with 100 μM ACh

(*left*) to give a macroscopic current. It was then perfused with MOR2 for 5 min (with no ACh), incubated in MOR2 for 45 min and afterward voltage-clamped again under the same conditions (*right*). In Fig. 6*B* an oocyte expressing the wild type nAChR was voltage-clamped at −70 mV and perfused with 100 μM ACh (*left*) to give a macroscopic current. Then it was perfused with MOR2 for 5 min (with no ACh) and exposed to methyl-β-cyclodextrin for 45 min and voltage-clamped again under the same conditions (−70 mV, 100 μM ACh) (*right*). As shown in Fig. 6*E*, exposure of an oocyte expressing the wild type AChR to methyl-β-cyclodextrin, which leads to a range between 17 and 46% with an average of 43% of decrease in the plasma membrane cholesterol levels (C/P = 0.3), does not seem to affect the wild type. Fig. 6 (*C* and *D*) shows the same experiments, including the control (*C*) for oocytes expressing the αC418W mutant. As shown in Fig. 6*D*, the αC418W shows a significant increase in macroscopic response after the depletion protocol. It is remarkable that this increase in macroscopic current response is caused by a single amino acid replacement at the lipid protein interface. Fig. 6*F* shows the average response of cholesterol depletion experiments for the αC418W mutant and its relation to control experiments. To estimate the net increase in the macroscopic response after cholesterol depletion, we estimated the difference between the potentiation in macroscopic response between the experimental and control oocytes. For the wild type the difference is less than 5% whereas for the αC418W mutant the potentiation effect is 67%.

To further characterize the effect of cholesterol depletion on nAChR function we constructed dose-responses curves before and after cholesterol depletion experiments (Fig. 7). After cholesterol depletion, the dose-response curve of the wild type
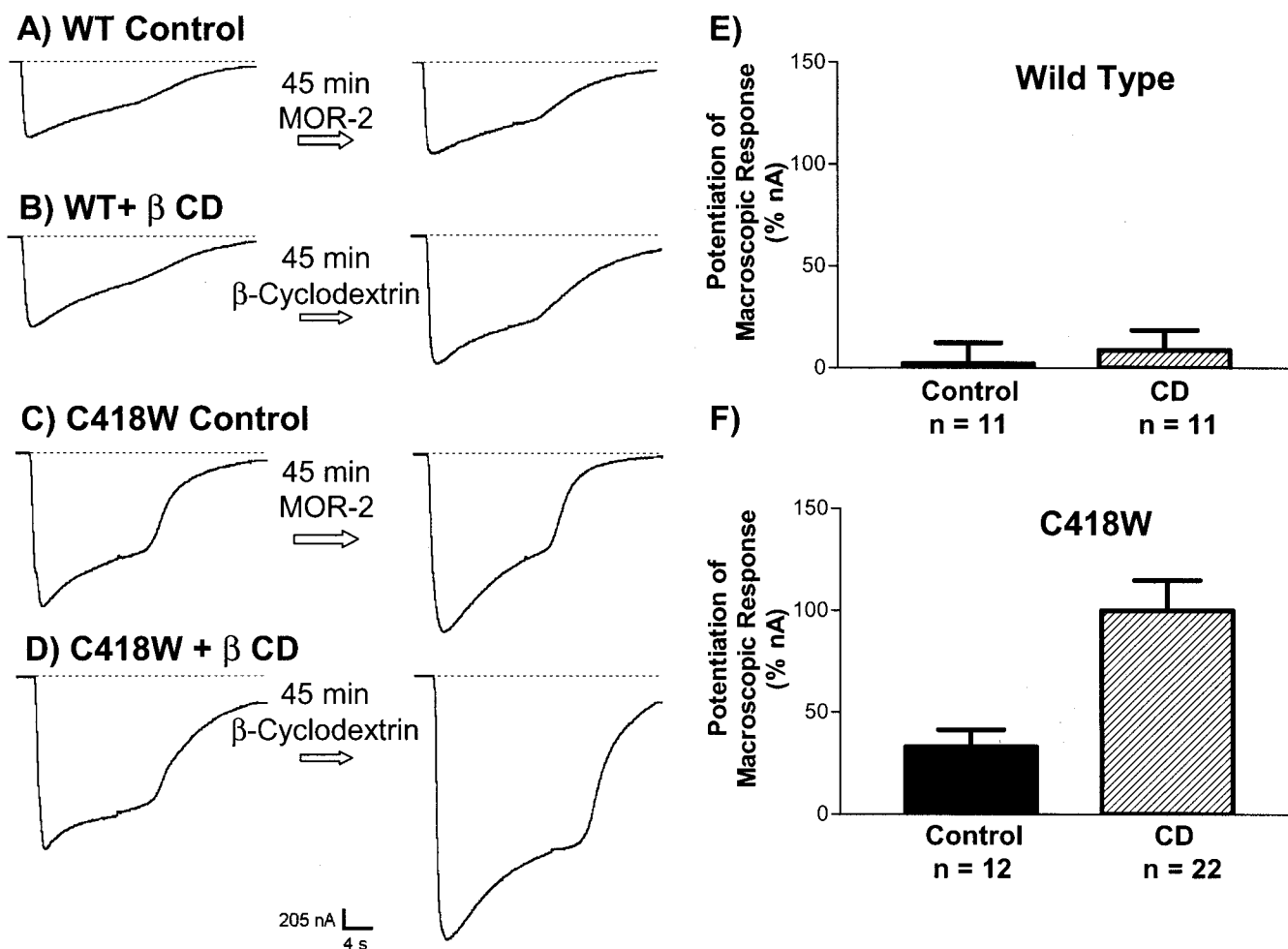
FIG. 6. **Cholesterol depletion produces an increase of the macroscopic response.** Current traces were recorded at 100 μM ACh, -70mV before (*left*) and after (*right*) 45 min of methyl-β-cyclodextrin exposure. In oocytes expressing wild type AChR (*A* and *B*), the average current after cholesterol depletion increased by 6.6%, as estimated from the difference between the experimental and control oocyte values (cholesterol-depleted 8.6–2.0% control; $n = 11$) (*E*). In oocytes expressing the αC418W AChR (*C* and *D*), the average current after cholesterol depletion was 66% (100% cholesterol-depleted -34% control; $n = 22$) (*F*). Note that the increase of macroscopic response is more dramatic in the mutant αC418W. The C/P molar ratio in control oocytes is 0.51 and 0.30 in the cholesterol-depleted oocytes.

remains very similar to that of the control (Fig. 7*A*), suggesting that a reduced number of channels, rather than inhibition of the channel gating mechanism, caused the observed effects. The average EC$_{50}$ value of the control oocytes expressing wild type AChR before and after depletion was 23 and 18 μM, respectively ($n = 4$ oocytes). In contrast, the EC$_{50}$ of the αC418W shifted from 4.2 μM (control) to 0.9 μM ($n = 5$ oocytes) after cholesterol depletion (Fig. 7*B*). The experimental data strongly suggest that cholesterol depletion did not produce any significant effects on the *Torpedo* wild type, whereas in a cholesterol-depleted environment the αC418W mutation displayed a significant gain in function response.

Cholesterol Enrichment and Depletion—These experiments were designed to examine if the inhibition detected in cholesterol enrichment experiments could be reversed by treating the oocytes with methyl-β-cyclodextrin. Oocytes expressing wild type or the αC418W mutation were perfused with 100 μM ACh and then exposed to cholesterol enrichment. The macroscopic response was assessed using voltage clamping with 100 μM ACh immediately after cholesterol enrichment (C/P = 0.87). Methyl-β-cyclodextrin (50 μM) in MOR2 was applied for 45 min after which the macroscopic response was measured at 100 μM ACh (Fig. 8). We estimate that this protocol removes 14% of the excess cholesterol (Fig. 2) and the C/P molar ratio was 0.75, higher than in a control oocyte (C/P = 0.51). Typical macro-

scopic currents obtained from these experiments for the wild type and αC418W mutant are shown in Fig. 8, *A* and *B*, respectively. Cholesterol enrichment reduced the wild type response by 79.7% ($n = 8$), and after a 14% depletion there was no significant change in the macroscopic response of the wild type. The same treatment in the αC418W mutant reduced the macroscopic current by 62.3% ($n = 12$), but after cholesterol depletion (Fig. 8*B*), 63% of the original current was recovered.

DISCUSSION

Previous biophysical studies of the nAChR used cholesterol as a probe for the study of lipid-protein interactions. In this study we examined the functional response of the *T. californica* AChR in different cholesterol environments in *Xenopus* oocytes. To assess the role of protein-lipid interactions on the AChR function, we used the novel lipid-exposed αC418W mutation that is located at the center of the M4 transmembrane segment of the alpha subunit (Fig. 9). The M4 is the most hydrophobic among the four membrane-spanning domains of the nAChR and has the lowest level of side-chain conservation. Photoaffinity labeling experiments have shown that M4 has the largest number of lipid-exposed residues (31), and the pattern of 3-trifluoromethyl-3-*m*-[^{125}I]iodophenyldiazirine labeling on the M4 domain is compatible with an α helical structure (32). We have shown that tryptophan substitutions at this
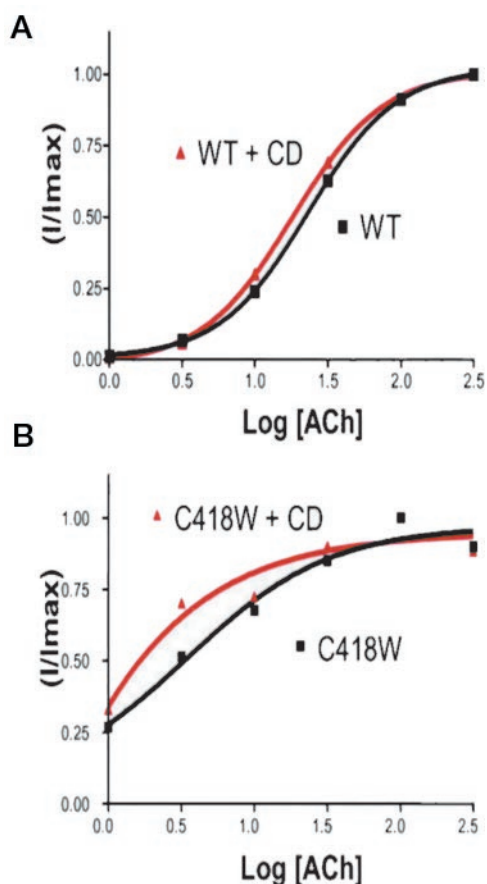
FIG. 7. **Cholesterol depletion reduced the αC418W EC₅₀.** The ACh concentrations used for the generation of dose-response curves were 1.0, 3.0, 10, 30, 100, and 300 μM ACh at −70 mV. After cholesterol depletion (C/P = 0.3) the dose-response curve of the WT (*A*) remains very similar to the control (23.0 ± 0.5 μM to 18.0 ± 0.8 μM; *n* = 4). In contrast, the EC₅₀ of the αC418W (*B*) shifted from 4.2 ± 0.3 μM (control) to 0.9 ± 0.1 μM after this moderate cholesterol depletion (*n* = 5).

postulated lipid-exposed αC418 position of the nAChR could produce a dramatic reduction in the closing transition of the internal ion channel leading to a dramatic gain-in-function response (19–21, 33). These studies raised the hypothesis that a unique interaction of the tryptophan side chain at the lipid interface of the receptor might alter nAChR function. In this study we examined the functional effect of cholesterol on this novel lipid-exposed mutation.

Numerous studies of lipid effects on the nAChR structure and function have demonstrated that membrane lipid composition can modulate receptor function (5, 27, 34–37). However, few studies have examined the effect of cholesterol on AChR function in an intact cell membrane (26, 27, and 38). The aim of this study was to measure the role of cholesterol on nAChR function with particular attention to lipid-protein interactions without compromising the physical state of the oocyte. The significant changes in the C/P molar ratios that we produced in the oocyte could represent a state of abnormal cholesterol levels in a natural cell membrane.

Cholesterol Enrichment and AChR Function—When the C/P molar ratio of an oocyte was increased to about 0.87, the macroscopic response of the *Torpedo* wild type was reduced to 51% (see Fig. 4). In contrast, the αC418W mutant displayed a higher state of inhibition: 81% of the macroscopic response was inhibited by cholesterol enrichment. It is remarkable that a single amino acid replacement in a lipid-exposed position of a membrane protein that has twenty transmembrane domains could produce such an increase in the sensitivity to levels of

cholesterol in the membrane. These results suggest that replacement of a tryptophan side chain at position αC418 increased the sensitivity of the nAChR function to the inhibitory effect of cholesterol.

Previous experiments in reconstituted *Torpedo* nAChR have demonstrated that the number of nAChRs that open in response to high agonist concentrations increases with the percentage of cholesterol in the bilayer, reaching a maximum at 30% molar cholesterol (17). This value corresponds to a C/P molar ratio of about 0.42, which is slightly lower than the molar ratio of *Xenopus* oocyte plasma membrane (C/P = 0.51). The C/P molar ratios reached after cholesterol enrichment in the oocyte membrane are much higher than those used in the studies of reconstituted *Torpedo* nAChR. Therefore, the state of inhibition that we observed at C/P molar ratios ≅ 0.87 in the wild type does not challenge the data from the reconstitution system. The higher C/P molar ratio range that we reached in oocytes suggests that the functional response of the *Torpedo* wild type in response to the membrane cholesterol levels or "bulk fluidity" might have a bell-shaped profile. The substitution of a tryptophan side chain at the αC418 position results in a displacement of this bell-shaped profile to lower C/P molar ratios, which leads to a loss-in-function response.

Cholesterol Depletion and AChR Function—The aim of these experiments was to examine the functional response of the nAChR in a reduced cholesterol environment, which presumably leads to a state of higher membrane fluidity. We depleted moderate cholesterol amounts from oocyte membranes to reach C/P molar ratios of 0.3 after 45 min of incubation. Under these conditions, *Torpedo* wild type exhibited no significant change in macroscopic response (Fig. 6, *A*, *B*, and *E*). This result was predictable because, as previously mentioned, the maximum response of the reconstituted *Torpedo* reached an optimal value at C/P molar ratios of 0.42. Therefore, at a C/P value of 0.3, the functional response of the *Torpedo* in reconstituted membrane is in its rising phase. In contrast, the same cholesterol depletion level produced a dramatic increase in the macroscopic response of the novel αC418W mutation (Fig. 6, *C*, *D*, and *F*) and a significant reduction in the EC₅₀, from 4.2 to 0.9 μM after cholesterol depletion (Fig. 7*B*). These results raised several questions: Why does a lipid-exposed mutation produce activation after cholesterol depletion? Does cholesterol depletion cause an increase in the open channel probability of the αC418W or an increase in the active pool of AChRs in the plasma membrane? What types of interactions govern this increase in current response of the αC418W after cholesterol depletion?

Cholesterol Enrichment and Depletion—The aim of these experiments was to investigate whether the inhibition caused by cholesterol enrichment could be reversed. After recording the current in the cholesterol-enriched state (C/P = 0.87), the oocyte was submitted to the depletion protocol. This depletion removed a small fraction of the excess cholesterol (14%). The average C/P molar ratio on these oocytes was 0.75, which is somewhat higher than in the normal oocyte (0.51). The current traces in Fig. 8*A* corresponding to *Torpedo* wild type showed no reversion of the inhibition. In contrast, identical experiments in oocytes expressing the αC418W mutation showed a significant recovery from inhibition (Fig. 8*B*). The recovery of the αC418W mutation after depleting a significant fraction of the excess cholesterol demonstrates that the interaction of this mutation with cholesterol is remarkably different from the wild type.

The role of cholesterol in modulating the dynamic properties of the lipid bilayer has been extensively studied, however, its role in lipid-protein interactions is less well understood. In
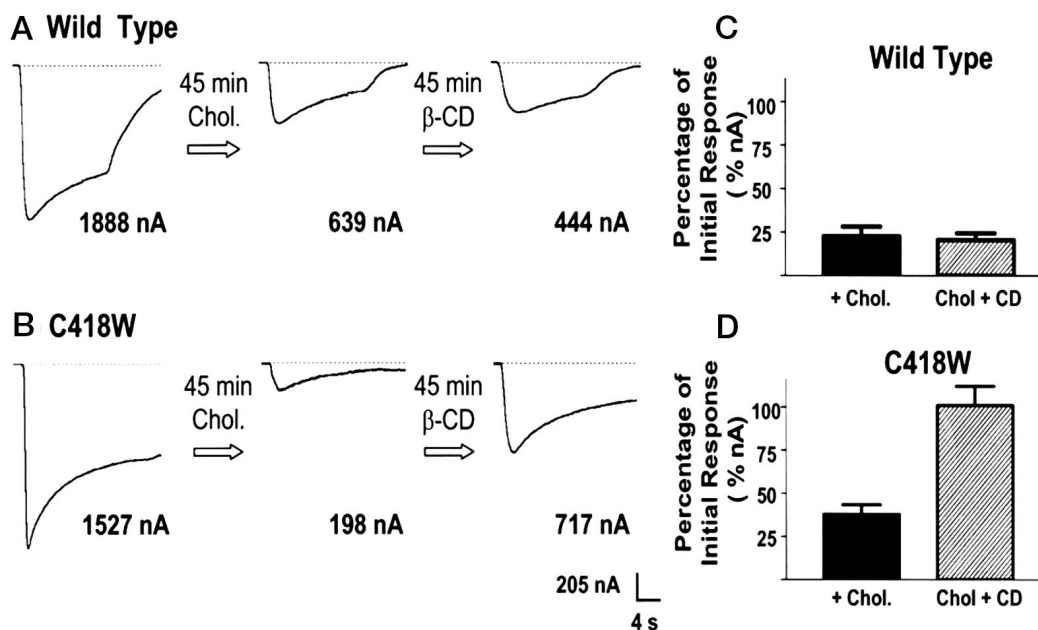
FIG. 8. **The αC418W mutant recovers from inhibition by cholesterol.** Oocytes expressing wild type (*top*) (*A*) and the αC418W mutant (*B*) were first perfused with 100 μM ACh (at −70 mV) and then exposed to a 45-min period of cholesterol enrichment followed by 45 min of cyclodextrin exposure. The amount of current in nanoamps for each step is indicated *below* the macroscopic current trace. The percentage of the initial response after cholesterol enrichment (C/P = 0.87) (+ *Chol bar*) for WT was 20.4% (*n* = 8) (*C*) and 37.8% for the αC418W mutant (*n* = 12) (*D*). After depletion of a fraction of the overloaded cholesterol, the average C/P ratio of the oocytes tested was 0.75. The WT did not recover (26.1% of the original current (*n* = 8, *Chol + CD* in *C*) from the inhibition by cholesterol whereas the C418W mutation recovered 63% of the original current (*n* = 12, *Chol + CD* in *D*) after this moderated cholesterol depletion. Control experiments in the absence of CD showed some degree of recuperation for the αC418W that was not observed for wild type.
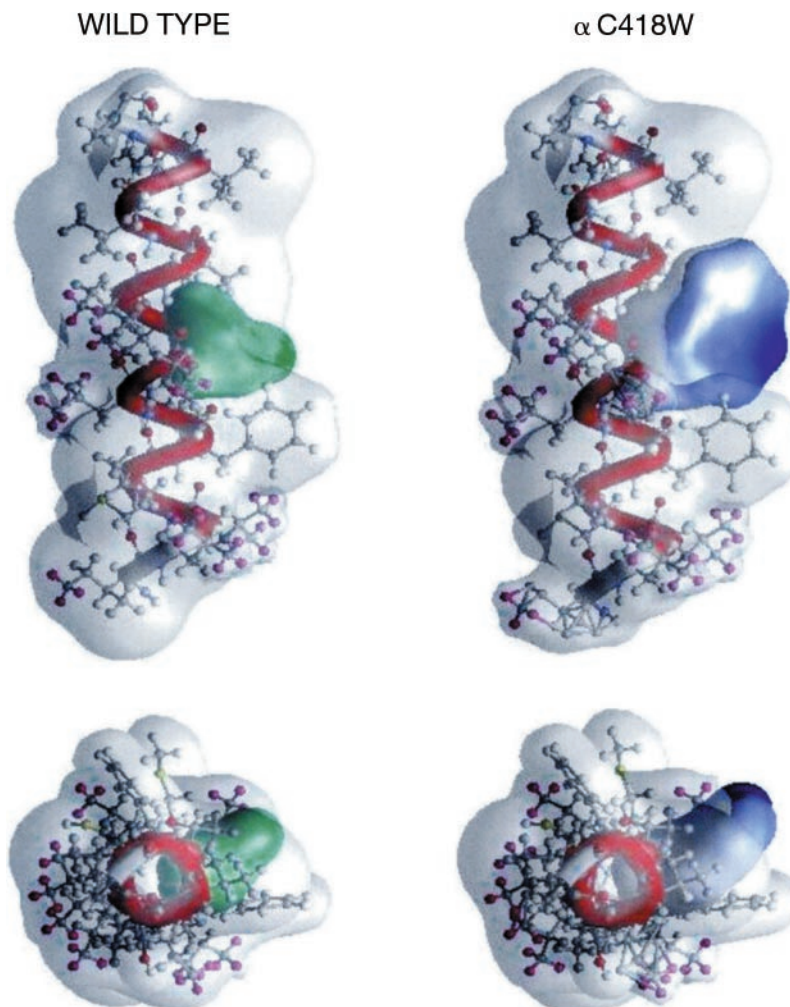
FIG. 9. **Molecular model of the alpha-M4 transmembrane domain of the *T. californica* AChR as an α-helical structure.** The localization of position αC418 in the M4 transmembrane segment is shown in a lateral and top view for the wild type (*left*) and the αC418W mutant (*right*). The volume of positions αC418 and αC418W are represented with *green* and *blue* density, respectively.

reconstituted membranes, the ability of the *Torpedo* nAChR to conduct cations across the membrane and undergo conformational transitions, from the resting to the desensitized state (R ⇒ D), is very sensitive to the lipid composition (8–10, 13, 17, 18, 39). When *Torpedo* nAChR was reconstituted into lipid bilayers lacking cholesterol, agonist cannot stimulate cation flux. However, the mechanism by which cholesterol regulates the conformational transitions of the nAChR remains unclear. Previous hypotheses have postulated two possible mechanisms to explain the effect of cholesterol on the modulation of AChR function. The first hypothesis proposes that the action of cholesterol on the nAChR might be associated with the bulk-lipid bilayer fluidity (9, 11, 13). A second hypothesis suggested that cholesterol may act as an "allosteric effector" at some nonannular or interstitial binding sites located within the protein, which are distinct from the lipid-protein interface (12, 14, 15, 40).

Role of Membrane Lipid Composition on the Conformational Equilibrium of the nAChR (*Fluidity Hypothesis*)—In this model an increase in membrane fluidity (reduced cholesterol) leads to a shift in nAChR (via an intermediate state) toward the desensitized state (D) (13). This hypothesis is in agreement with our data from the cholesterol depletion experiments for the *Torpedo* wild type. However, it does not explain the increase in macroscopic response observed for the αC418W mutation. Why does a reduction in cholesterol level lead to activation of a lipid-exposed mutation? For the αC418W mutation, the fluidity model works in the opposite direction. In high fluidity we observed a higher degree of activation. This increase in macroscopic response might be caused by a gain in function response and/or an increase in the resting (R) pool of nAChR. A very attractive hypothesis is that the opening transition of the αC418W is facilitated in a more fluid environment due to penetration of the tryptophan side chain in the bilayer, leading to a more stable open-channel state. Another hypothesis is that the equilibrium between resting and desensitized states of the nAChR is very sensitive to cholesterol levels in the membrane, and higher cholesterol levels in both cases decrease the active resting pool of receptors. It is also remarkable that the αC418W mutation recovered from the inhibitory effect at high levels of cholesterol when the C/P molar ratio was restored close to the normal value. In contrast, the wild type did not recover from the inhibitory effects at high levels of cholesterol. Therefore, substitution of a tryptophan side chain at a single lipid-exposed mutation produced an nAChR that is much more sensitive to cholesterol than the wild type receptor. The present data suggest that the mechanism by which cholesterol modulates AChR function might involve specific structural interactions or perhaps specific orientations of the transmembrane domains that are exposed toward the lipid environment. Based on the estimation of the energetic contribution of the tryptophan side chain to the closing channel rate, one of the hypotheses was that a tryptophan could interact with the lipid interface via Van der Waals or dipole interactions at the periphery of the nAChR. Based on this hypothesis and the present data, it is reasonable to speculate that the tryptophan residue at position αC418 could be altering normal interactions of the nAChR with cholesterol leading to the observed increase in sensitivity to the membrane cholesterol levels. Along this line of thinking, future studies with different side chains at the αC418 will be needed to define the functional role of these interactions. The present data suggest that the dramatic differences in the functional modulation of cholesterol that we observed between the *Torpedo* wild type and the αC418W mutation are governed by specific interactions of the lipid-exposed domains of the nAChR with the membrane lipid bilayer.

Conclusions—In summary, the present work represents a new approach to elucidate the molecular mechanisms of the interaction of cholesterol with the nAChR. The present data suggest that cholesterol may be acting on the *Torpedo* wild type via a complex regulatory mechanism that controls the equilibrium between the silent and functional surface pools of nAChRs. Further evidence that the movement of receptors from the silent and functional surface pools of nAChRs is modulated by membrane lipid composition will represent a novel mechanism of nAChR regulation. The modulation of cholesterol on the αC418W function is dramatically different from wild type: 1) at lower cholesterol the C418W shows a gain-in-function response that could be due to increased levels of nAChRs or a gain-in-function of channel activity, 2) at high cholesterol levels higher inhibition is observed, and 3) the inhibition caused by higher C/P molar ratios could be reversed. Further experiments at the single channel level will define which of these mechanisms is responsible for the observed effects on the αC418W. It is conceivable that integral membrane proteins like the nAChR have an intrinsic bell-shaped response to membrane cholesterol levels and that structural and/or dynamic interactions at the periphery of the protein-lipid interface can displace or modulate these bell-shaped profiles to states of lower or higher activation. Perhaps low levels of side-chain conservation on the lipid-exposed domains among the nAChR species have evolved to provide the structural adaptations for different lipid environments. These new approaches demonstrate that lipid replacement in oocytes is feasible, and development of these methods will open a new avenue to the study of structural and functional aspects of lipid-protein interactions on ion channel function in a common expression system.

REFERENCES

1. Arias, H. B. (1998) *Biochim. Biophys. Acta* **1376,** 173–220
2. Changeux, J. P., and Edelstein, S. J. (1998) *Neuron* **21,** 959–980
3. Karlin, A., and Akabas, M. H. (1995) *Neuron* **15,** 1231–1244
4. Galzi, J. L., Revah, F., Bessis, A., and Changeux, J. P. (1991) *Annu. Rev. Pharmacol.* **31,** 37–42
5. Pradier, L., and McNamee, M. G. (1992) in *The Structure of Biological Membranes* (Yeagle, P., ed) pp. 1047–1106, Telford Press, Caldwell, NJ
6. Unwin, N. (1993) *J. Membr. Biol.* **229,** 1101–1124
7. Dipaola, M., Czajkowski, C., and Karlin, A. (1989) *J. Biol. Chem.* **264,** 15457–15463
8. Ochoa, E. L., Dalziel, A. W., and McNamee, M. G. (1983) *Biochim. Biophys. Acta* **727,** 151–162
9. Fong, T. M., and McNamee, M. G. (1986) *Biochemistry* **25,** 830–840
10. Méthot, N., and Baenziger, J. E. (1998) *Biochemistry* **37,** 14815–14822
11. Sunshine, C., and McNamee, M. G. (1994) *Biochim. Biophys. Acta* **1108,** 240–246
12. Fernandez-Ballester, G., Castresana, J., Fernández, A. M., Arrondo, J. L., Ferragut, J. A., and González-Ros, J. M. (1994) *Biochem. Soc. Trans.* **22,** 776–780
13. Baenziger, J. E., Morris, M. L., Darsaut, T. E., and Ryan, S. E. (2000) *J. Biol. Chem.* **275,** 777–784
14. Narayanaswami, V., and McNamee, M. G. (1993) *Biochemistry* **32,** 12420–12427
15. Jones, O. T., and McNamee, M. G. (1988) *Biochemistry* **27,** 2364–2374
16. Corbing, J., Wang, H. H., and Blanton, M. P. (1998) *Biochim. Biophys. Acta* **1414,** 65–74
17. Rankin, S. E., Addona, G. H., Kloczewiak, M. A., Bugge, B., and Miller, K. W. (1997) *Biophys. J.* **73,** 2446–2455
18. Raines, D. E., and Krishnan, N. S. (1998) *Biochemistry* **37,** 956–964
19. Lee, Y. H., Li, L., Lasalde, J. A., Rojas, L., McNamee, M. G., Ortiz-Miranda, S. I., and Pappone, P. (1994) *Biophys. J.* **66,** 646–653
20. Ortiz-Miranda, S. I., Lasalde, J. A., Pappone, P. A., and McNamee, M. G. (1997) *J. Membr. Biol.* **158,** 17–30
21. Tamamizu, S., Lee, Y. H., Hung, B., McNamee, M. G., and Lasalde-Dominicci, J. A. (1999) *J. Membr. Biol.* **170,** 157–164
22. Ohlsson, R. I., Lane, C. D., and Guengerich, F. P. (1981) *Eur. J. Biochem.* **115,** 367–373
23. Johnson, S. M. (1979) *Anal. Biochem.* **95,** 344–350
24. Richmond, W. (1973) *Clin. Chem.* **19,** 1350–1356
25. Ohtani, Y., Irie, T., Uekama, K., Fukunaga, K., and Pitha, J. (1989) *Eur. J. Biochem.* **186,** 17–22
26. Christian, A. E., Haynes, M. P., Phillips, M. C., and Rothblat, G. H. (1997) *J. Lipid Res.* **38,** 2264–2272

27. Lasalde, J. A. (1992) in *Membrane Proteins: Structures, Interactions and Models* (Pullman, A., *et al.*, eds) pp. 199–212, Kluwer Academic Publishers, Norwell, MA
28. Lasalde, J. A., Colom, A., Resto, E., and Zuazaga, C. (1995) *Biochim. Biophys. Acta* **1235,** 427–438
29. Barish, M. E. (1983) *J. Physiol.* (*Lond.*) **342,** 309–325
30. Mishina, M., Kurosaki, T., Tobimatsu, T., Morimoto, Y., Noda, M., Yamamoto, T., Terao, M., Lindstrom, J., Takahashi, T., Kuno, M., and Numa, S. (1984) *Nature* **307,** 604–608
31. Blanton, M. P., and Cohen, J. B. (1992) *Biochemistry* **31,** 3738–3750
32. Blanton, M. P., and Cohen J. B. (1994) *Biochemistry* **33,** 2859–2872
33. Tamamizu, S., Guzmán, G. R., Santiago, J., Rojas, L., McNamee, M. G., and Lasalde-Dominicci, J. A. (2000) *Biochemistry* **39,** 4666–4673
34. Fong, T. M., and McNamee, M. G. (1987) *Biochemistry* **26,** 3871–3880
35. Bhushan, A., and McNamee, M. G. (1993) *Biophys. J.* **64,** 716–723
36. Barrantes, F. J. (1997) in *From Ion Channels to Cell-to Cell Conversations* (Latorre, R., and Saenz, J. C., eds) pp. 199–216, Plenum Press, New York
37. Zanello, L. P., Aztiria, E., Antollini, S., and Barrantes, F. J. (1996) *Biophys. J.* **70,** 2155–2164
38. Lechleiter, J., Wells, M., and Grunner, R. (1986) *Biochim. Biophys. Acta* **856,** 640–645
39. Barrantes, F. J. (1993) in *Protein-Lipid Interactions* (Watts, A., ed) pp. 231–257, New Comprehensive Biochemistry, Vol. 26, Elsevier, Amsterdam
40. Antollini, S. S., and Barrantes, F. J. (1998) *Biochemistry* **37,** 16653–16662
41. Lasalde, J. A., Tamamizu, S., Butler, D. H., Vibat, C. R. T., Hung, B., and McNamee, M. G. (1996) *Biochemistry* **35,** 14139–14148